

**Methods of Spectral Reflectance Reconstruction for  
A Sinarback 54 Digital Camera**

**Yonghui Zhao**

**Lawrence A. Taplin**

**Mahdi Nezamabadi**

**Roy S. Berns**

**Munsell Color Science Laboratory**

**Chester F. Carlson Center for Imaging Science**

**Rochester Institute of Technology**



**December, 2004**

## **Abstract**

There is an urgent need to build digital image databases with adequate colorimetric accuracy for museums, archives and libraries. Traditional colorimetric imaging suffers from the possibilities of metameric problem, while spectral imaging can facilitate accurate tristimulus estimation and possibilities for spectral reconstruction of each pixel. Spectral image archives can be used to render accurate images both spectrally and colorimetrically to the original target for any illuminant and observer. The most convenient and practical capture system for spectral imaging combines a commercial trichromatic camera with two absorption filters to define image spectrally. Two images were taken for each target; so six-channel multichannel images were obtained. Three methods of spectral color reproduction were evaluated: pseudoinverse method, canonical correlation regression (CCR), and Matrix R method. The CCR method can obtain the highest spectral accuracy among these methods, just because it incorporates fifteen cross product terms in the simulation. The Matrix R method can reach the same spectral accuracy as the pseudoinverse method, and the spectral accuracy of both methods could be improved if they also use the same cross product terms. On the other hand, the Matrix R can achieve the best colorimetric accuracy for a certain combination of illuminant and observer. Thus, the Matrix R is a very promising method for achieving artwork images with sufficient spectral and colorimetric accuracy.

## **I. Introduction**

Imaging is an important technique for visual documentation of art. There is an urgent need to build digital image databases with adequate colorimetric accuracy for museums, archives, and libraries. Traditional color-acquisition devices capture spectral signals by acquiring only three samples, critically under-sampling the spectral information and suffering from the possibilities of metamerism. On the other hand, spectral devices

increase the sampling and can reconstruct spectral information of each scene pixel. This process is called spectral reflectance reconstruction. Retrieving spectral reflectances of each pixel is highly desirable, since spectral information can be used to render the images under any virtual illuminant for any observer. The advantages of spectral image archives have been summarized by Berns. <sup>[1]</sup>

The existing reconstruction techniques can be classified in three paradigms: <sup>[5]</sup> direct reconstruction, reconstruction by interpolation, and indirect reconstruction or learning-based reconstruction. First, direct reconstruction is based on the inverse of the camera model, in which camera signals are the integral of spectral power distribution of light source, camera spectral sensitivities, detector spectral response and spectral reflectance of object surface. The solution is not stable due to the effect of noise. The camera model is not complete unless the noise is characterized. Because of difficulties associated with the characterization of the noise, the technique isn't popular. Nevertheless, virtual camera model is created for selecting optimal filters for multispectral imaging or for testing hierarchical cluster analysis of spectral imaging. <sup>[6]</sup> Second, the camera responses can be interpolated to find an approximation of the corresponding reflectance, and therefore the method is called reconstruction by interpolation. <sup>[4]</sup> In the European project CRISATEL (Conservation Restoration Innovation System for Imaging capture and Digital Archiving to Enhance Training Education and Lifelong Learning) a spectral acquisition system has 10 interference filters in visible range and 3 in the near-infrared range. Spectral reflectance reconstruction is

achieved by a simple cubic spline interpolation between measured points. The system exhibits high spectral and colorimetric accuracy.

Finally, indirect reconstruction is also called learning-based reconstruction. It means that a calibration target is needed to find the relationship between camera signals and spectral reflectance, and after that, the camera signals of independent targets can be transferred into spectral reflectance. A multi-year research program in Munsell Color Science Laboratory (MCSL) has been developed to implement many methods of spectral color reproduction based on this learning processing.<sup>[7,8]</sup> Three multispectral acquisition systems have been undergone testing: 31 liquid-crystal tunable filters with a monochrome camera, six absorption filters with a monochrome camera, and two absorption filters with a commercial color-filter-array (CFA) camera. The last system is the most practical system, since its main part is a commercial RGB digital camera. The two absorption filters are selected according to computer simulation using a virtual camera model. This capture system is tested and the results are summarized in this report.

Two sets of RGB images were acquired by sequentially placing the two filters in the optical path for each target, providing six-channel camera signals. Three spectral imaging methods were implemented, and they are pseudoinverse method, Matrix R method and canonical correlation regression (CCR), which will be discussed in the next section. The three-channel production camera signals are also used to develop a 3-by-3 method only for comparative purposes.

## II. Methods

One colorimetric imaging method and three spectral imaging methods are briefly introduced in this section. A commercial color-filter-array (CFA) camera was tested, and the three-channel camera signals can be transformed to tristimulus values using a colorimetric method by an optimized 3-by-3 matrix. On the other hand, the CFA camera was coupled with a pair of absorption filters, yielding six channels, and the six-channel camera signals can be transformed to spectral reflectance factors using three spectral imaging methods – pseudoinverse method, Matrix R method and canonical correlation regression.

### 1. The 3-by-3 Matrix

The three-channel camera signals are first linearized to luminance factors using Gain-Offset-Gain (GOG) model, and then transformed to tristimulus values,  $\mathbf{T}_c$ , by a 3-by-3 matrix,  $\mathbf{M}_c$ .

$$\mathbf{D}_{L,i} = (\alpha_i \mathbf{D}_i + \beta_i)^{\gamma_i} \quad i = 1, 2, 3 \quad (1)$$

$$\mathbf{T}_c = \mathbf{M}_c \times \mathbf{D}_L \quad (2)$$

$\mathbf{D}_i$  and  $\mathbf{D}_{L,i}$  are raw and linearized camera signals for the  $i$ -th channel,  $\alpha_i$ ,  $\beta_i$  and  $\gamma_i$  are the gain, offset and gamma for the channel, respectively. Nonlinear optimization was used to derive transformation matrix  $\mathbf{M}_c$  and nine parameters for GOG model with three parameters – gain, offset and gamma for each channel. The objective function was to minimize the weighted sum of mean and maximum color difference CIEDE2000 for the calibration target.

## 2. The Pseudoinverse Method

The six-channel camera signals were transformed to spectral reflectance factors using a transformation matrix. The transform matrix,  $\mathbf{T}$ , is constructed by a generalized pseudo-inverse method based on Singular Value Decomposition (SVD), as shown in Eq. (3):

$$\mathbf{T} = \mathbf{R} \times \text{PINV}(\mathbf{D}) \quad (3)$$

where  $\mathbf{R}$  is spectral reflectance factors of the calibration samples,  $\text{PINV}$  is the pseudoinverse function, available from Matlab, and  $\mathbf{D}$  is the corresponding camera signals of the calibration samples. Then, predicted spectral reflectance factors,  $\hat{\mathbf{R}}$ , can be calculated using matrix multiplication for both calibration and verification targets.

$$\hat{\mathbf{R}} = \mathbf{T} \times \mathbf{D} \quad (4)$$

## 3. The Matrix R Method

Spectral reflectance factors are estimated based on the Wyszecki hypothesis that any stimulus can be decomposed into a fundamental stimulus and a metameric black. The mathematical technique of the hypothesis, known as Matrix R, was developed by Cohen and Kappauf. [2,3]

First, as illustrated in the left branch of the flowchart, spectral reflectance factor is estimated from camera signals using a transformation matrix,  $\mathbf{T}$ , which is the same transformation matrix as that for the pseudoinverse method.

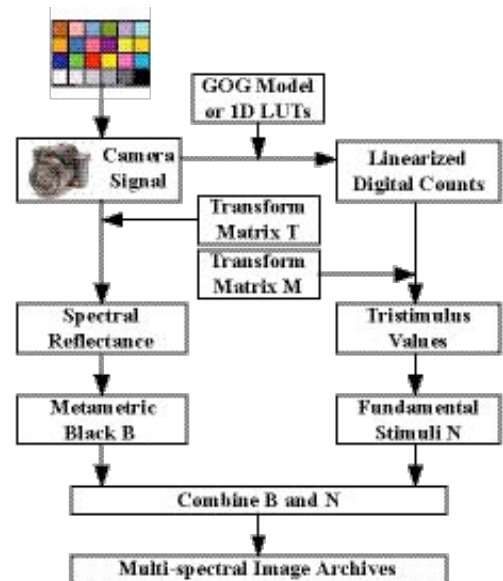


Figure 1 Flowchart of Matrix R method

Second, along the right branch of the flowchart, tristimulus values are predicted from camera signals using two steps – linearizing the signals related to luminous factor using the GOG model for each channel and transferring the linearized signals to tristimulus values. The difference between matrix R method and a 3-by-3 matrix is due to the transformation matrix,  $\mathbf{M}_c$ . For modified camera,  $\mathbf{M}_c$  was a  $3 \times 6$  matrix, while for production camera,  $\mathbf{M}_c$  was a  $3 \times 3$  matrix.

Finally, the metameric black from predicted spectral reflectance factors,  $\hat{\mathbf{R}}$ , will be fused with the fundamental stimulus from estimated tristimulus values,  $\mathbf{T}_c$ , to get hybrid spectral reflectance factors,  $\hat{\mathbf{R}}_c$ , as shown in Eq. (5):

$$\hat{\mathbf{R}}_c = \mathbf{A}(\mathbf{A}'\mathbf{A})^{-1}\mathbf{T}_c + (\mathbf{I} - \mathbf{A}(\mathbf{A}'\mathbf{A})^{-1}\mathbf{A}')\hat{\mathbf{R}} \quad (5)$$

where  $\mathbf{A}$  is a matrix of ASTM weights applicable to the combination of illuminant and observer and  $\mathbf{I}$  is an identity matrix.

#### 4. Canonical Correlation Regression (CCR)

A statistical method – canonical correlation analysis (CCA) is used to identify and quantify associations between two sets of variables for description purpose as well as for predicative purpose in canonical correlation regression (CCR). The detailed information about CCA and CCR can be found in Appendix II. The six-channel camera signals are expanded to 21-channel camera signals by adding 15 cross product terms. This operation is necessary in order to increase the number of input sets of variables to the CCR method. More details about this operation will be discussed later on. The wavelength range for spectral reflectance is from 380 nm to 730 nm at 10 nm increments, totaling 36 data values. The spectral reflectance can be estimated from the expanded camera signals by a  $36 \times 21$  matrix, expressed in Eq. (6):

$$\hat{\mathbf{X}}^{(2)} = (\mathbf{A}\mathbf{mat} \times \beta_{CC} \times \mathbf{B}\mathbf{mat}^{-1})^T \times \mathbf{X}^{(1)} \quad (6)$$

where  $\mathbf{X}^{(1)}$  is a matrix composed of 21-channel camera signals,  $\hat{\mathbf{X}}^{(2)}$  is an estimated matrix of spectral reflectance factors,  $\mathbf{A}\mathbf{mat}$  and  $\mathbf{B}\mathbf{mat}$  are two weight matrices, and  $\beta_{CC}$  is a matrix of canonical correlations between two sets of canonical variables.

### III. Experimental

A Sinarback 54 color-filter-array (CFA) digital camera was used in the experiment. The camera used a Kodak KAF-22000CE CCD with a resolution of  $5440 \times 4880$  pixels. Sinar Capture 4.1 software controlled its operation. The camera was modified in two ways. The build-in IR cut-off filter in the camera was removed and replaced with a Unaxis broadband near-infrared (NIR) blocking filter. Two absorption glass filters were selected

from a pool of Schott glass filters: BG39 and GG475. These two filters were placed sequentially in the optical path, and two sets of RGB images were taken for each target. The combination of the Unaxis and BG39 filter had almost the same spectral transmittance as the Sinar build-in IR cut-off filter, so one RGB image taken through the Schott BG39 filter could simulate the production camera and was transformed to tristimulus values by an optimized 3-by-3 matrix. The two RGB images provided six-channel camera signals, which were transformed to spectral reflectance factor using the three methods of spectral reconstruction described above.

The camera was set up approximately perpendicular to the target. The lighting system includes two Broncolor HMI F1200 sources, placed at both sides of the camera along the directions  $45^\circ$  away from the line between the camera and target.

Seven targets were evaluated: the GretagMacbeth ColorChecker DC, The GretagMacbeth ColorChecker, the ESSER TE221 scanner target, a custom target of Gamblin conservation colors, an acrylic-medium blue target with a number of different blue pigments, and two small oil paintings. The GretagMacbeth ColorChecker DC was used as the calibration target, and all the other targets were used as verification targets. For each oil painting, eleven measurement points were used. The spectral reflectance factors of the targets were measured using a Macbeth SpectroEye spectrophotometer with 45/0 geometry. The wavelength range was from 380 nm to 730 nm at 10 nm intervals. The nature of spectral reflectance of these targets is discussed in Appendix I.

## IV. Results and Discussions

### 1. The 3-by-3 Matrix

The fabricated RGB images can be transformed into tristimulus values by two ways. One is a simple 3-by-3 matrix obtained using pseudoinverse method without optimization, and the other includes three 1-D LUTs and an optimized 3-by-3 matrix, described in Section II. The results of color difference CIEDE2000 are summarized in Tables I and II. It can be seen that the nonlinear optimization process improved colorimetric accuracy. However, the maximum errors of the color difference were still large because of the inherent limitations of the sensor's spectral sensitivities restricting colorimetric performance.

Table I Statistics of color differences without optimization

CIEDE00	CCDC	CC	ESSER	BLUE	GAMBLIN	FISH	FLOWER	All Targets
Mean	2.5	2.8	3.4	4.7	3.3	5.1	5.4	3.2
Max	14.5	9.4	13.4	12.7	10.6	13.1	12.3	14.5
Std. Dev.	1.8	2.0	2.5	3.3	2.4	4.0	4.0	2.5

Table II Statistics of color differences with optimization

CIEDE00	CCDC	CC	ESSER	BLUE	GAMBLIN	FISH	FLOWER	All Targets
Mean	1.9	2.6	3.3	4.5	3.0	4.5	4.5	2.9
Max	10.9	9.2	13.2	12.5	10.7	13.4	12.4	13.4
Std. Dev.	1.9	2.0	2.3	2.9	2.3	3.5	3.3	2.4

## 2. Pseudoinverse Method

The transformation vectors from camera signals to spectral reflectance are plotted in Figure 2. The vector values at each wavelength represent quantitative contributions of spectral reflectance from the corresponding channels. These vectors are greatly affected by the spectral properties of the calibration target. An optimal calibration target should provide appreciable information for at least one channel at every wavelength. The current calibration target works quite well within the visible range, except for wavelengths at 380 nm, 390nm and 680 nm. Table III lists colorimetric and spectral accuracy comparing a conventional small-aperture *in-situ* spectrophotometer with the modified Sinarback 54 spectral image for the pseudoinverse method.

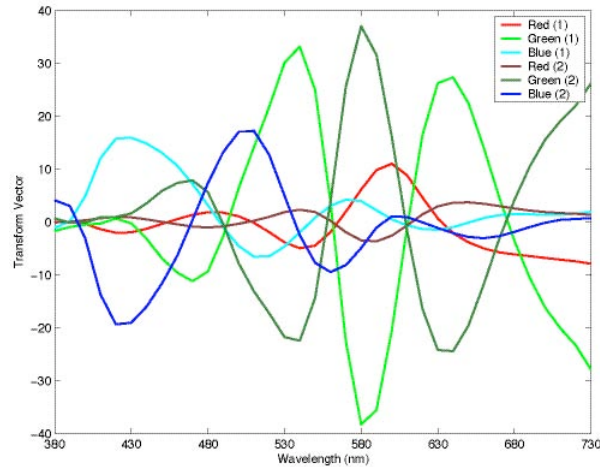


Figure 2 Transform vectors from camera signals to spectral reflectance

Table III Performance matrices comparing a conventional small-aperture *in-situ* spectrophotometer with modified Sinarback 54 spectral image for pseudoinverse method

	$\Delta E_{00}$ (D65, 2°)	RMS (%)	Metameric Index (D65 -> A, $\Delta E_{00}$ )	Metameric Index (A -> D65, $\Delta E_{00}$ )
ColorChecker DC				
Average	1.4	1.6	0.5	0.6
Maximum	13.3	4.0	5.0	6.5
Std. Dev.	1.6	0.6	0.8	0.9
ColorChecker				
Average	1.2	1.6	0.3	0.4
Maximum	3.5	2.6	1.4	1.7
Std. Dev.	0.9	0.6	0.4	0.4
ESSER				
Average	1.3	1.9	0.4	0.4
Maximum	5.3	6.8	3.3	2.4
Std. Dev.	0.9	1.0	0.4	0.4
Blue				
Average	3.2	3.6	1.1	1.0
Maximum	10.1	10.0	5.3	6.0
Std. Dev.	2.1	2.1	1.2	1.2
Gamblin				
Average	2.0	2.8	0.5	0.6
Maximum	4.3	8.5	2.0	2.8
Std. Dev.	0.9	1.5	0.4	0.6
Fish				
Average	2.3	2.6	0.7	0.7
Maximum	4.3	5.4	2.3	2.7
Std. Dev.	1.1	1.4	0.7	0.8
Flower				
Average	3.7	3.2	1.0	1.2
Maximum	9.3	8.8	7.5	8.3
Std. Dev.	2.5	2.0	2.2	2.4
All Targets				
Average	1.6	2.0	0.5	0.6
Maximum	13.3	10.0	7.5	8.3
Std. Dev.	1.5	1.2	0.7	0.8

### 3. Matrix R Method

The Matrix R method fuses the metameric black from pseudoinverse method and the fundamental stimulus from the nonlinear optimization for a certain combination of illuminant and observer. Table IV lists colorimetric and spectral accuracy comparing a

conventional small-aperture *in-situ* spectrophotometer with modified Sinarback 54 spectral image for the Matrix R method.

Table IV Performance matrices comparing a conventional small-aperture *in-situ* spectrophotometer with modified Sinarback 54 spectral image for the Matrix R method

	$\Delta E_{00}$ (D65, 2°)	RMS (%)	Metameric Index (D65 -> A, $\Delta E_{00}$ )	Metameric Index (A -> D65, $\Delta E_{00}$ )
ColorChecker DC				
Average	0.9	1.5	0.5	0.6
Maximum	3.0	3.9	5.0	5.9
Std. Dev.	0.7	0.6	0.8	0.8
ColorChecker				
Average	0.9	1.6	0.3	0.4
Maximum	2.2	2.6	1.4	1.5
Std. Dev.	0.5	0.6	0.4	0.4
ESSER				
Average	1.3	1.9	0.4	0.4
Maximum	4.2	6.9	3.3	2.4
Std. Dev.	0.8	1.0	0.4	0.3
Blue				
Average	2.4	3.6	1.1	0.9
Maximum	7.8	10.0	5.3	5.8
Std. Dev.	1.5	2.1	1.2	1.1
Gamblin				
Average	1.8	2.8	0.5	0.6
Maximum	3.9	8.5	2.0	2.7
Std. Dev.	0.8	1.5	0.4	0.6
Fish				
Average	2.8	2.5	0.7	0.7
Maximum	6.8	5.3	2.3	2.3
Std. Dev.	2.1	1.3	0.7	0.7
Flower				
Average	2.8	3.2	1.0	1.2
Maximum	6.3	8.7	7.5	7.8
Std. Dev.	1.8	2.0	2.2	2.2
All Targets				
Average	1.3	2.0	0.5	0.5
Maximum	7.8	10.0	7.5	7.8
Std. Dev.	1.0	1.2	0.7	0.7

#### 4. Canonical Correlation Regression (CCR)

Figure 3 plots the mean color difference CIEDE2000 and mean spectral % RMS error when the number of canonical variables increases. It can be seen easily that both mean color difference and spectral RMS errors are decreasing with increasing number of canonical variables, and remain almost unchanged when that number exceeds 16. So the optimal choice of the number of canonical variables is 16. Table V lists colorimetric and spectral accuracy comparing a conventional small-aperture *in-situ* spectrophotometer with modified Sinarback 54 spectral image using the CCR method.

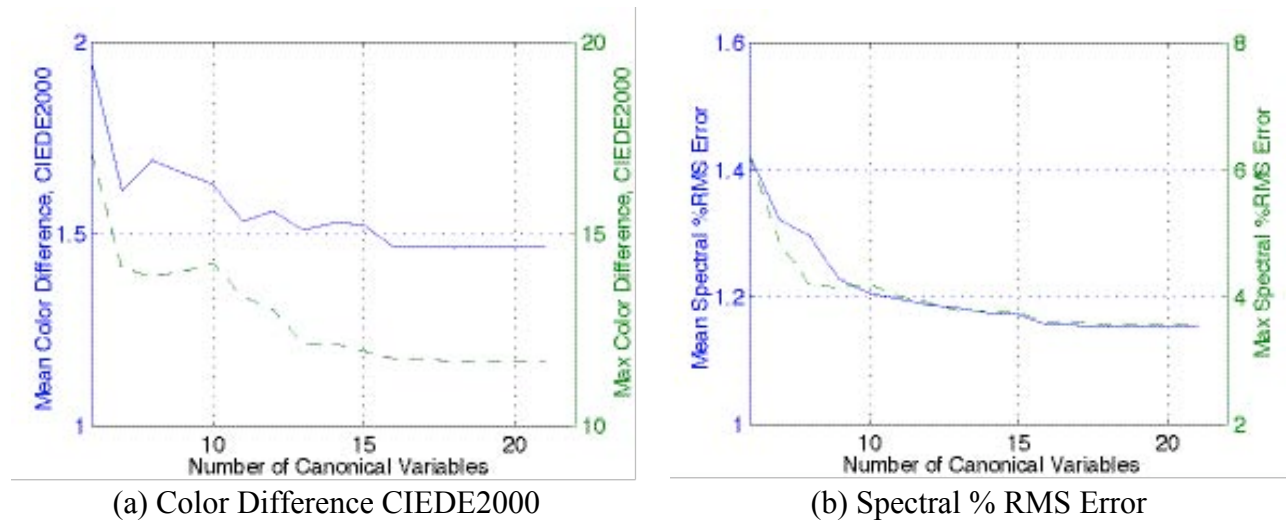


Figure 3 The dependence of color difference CIEDE2000 and spectral % RMS error on the number of canonical variables

Table V Performance matrices comparing a conventional small-aperture *in-situ* spectrophotometer with modified Sinarback 54 spectral image for CCR method

	$\Delta E_{00}$ (D65, 2°)	RMS (%)	Metameric Index (D65 -> A, $\Delta E_{00}$ )	Metameric Index (A -> D65, $\Delta E_{00}$ )
ColorChecker DC				
Average	1.5	1.2	0.5	0.7
Maximum	11.8	3.6	6.3	6.6
Std. Dev.	1.5	0.4	0.8	0.9
ColorChecker				
Average	1.4	1.4	0.4	0.5
Maximum	4.0	2.6	1.4	1.9
Std. Dev.	1.0	0.5	0.4	0.5
ESSER				
Average	1.3	1.6	0.4	0.4
Maximum	5.5	6.2	3.0	2.4
Std. Dev.	0.9	0.9	0.4	0.4
Blue				
Average	3.2	3.3	1.1	1.1
Maximum	10.5	8.3	5.3	6.2
Std. Dev.	2.1	1.5	1.2	1.2
Gamblin				
Average	2.0	2.4	0.6	0.7
Maximum	4.5	6.5	2.1	2.9
Std. Dev.	0.8	1.1	0.5	0.6
Fish				
Average	2.4	2.1	0.8	0.9
Maximum	4.5	5.0	2.9	3.7
Std. Dev.	1.0	1.1	0.8	1.0
Flower				
Average	2.9	2.7	1.1	1.4
Maximum	10.7	6.9	8.2	9.3
Std. Dev.	3.0	1.5	2.4	2.7
All Targets				
Average	1.6	1.7	0.5	0.6
Maximum	11.8	8.3	8.2	9.3
Std. Dev.	1.4	1.1	0.8	0.8

## 5. Comparison

The mean CIEDE2000 color differences for all the methods are plotted in Figure 4. The three spectral imaging methods are superior to the colorimetric methods. The nonlinear optimization is an effective technique to improve colorimetric performance of the camera. For example, the optimized 3-by-3-matrix method and the matrix R method are achieved higher colorimetric accuracy than the corresponding pseudoinverse methods. Among all the methods, the Matrix R method can result in the highest colorimetric accuracy.

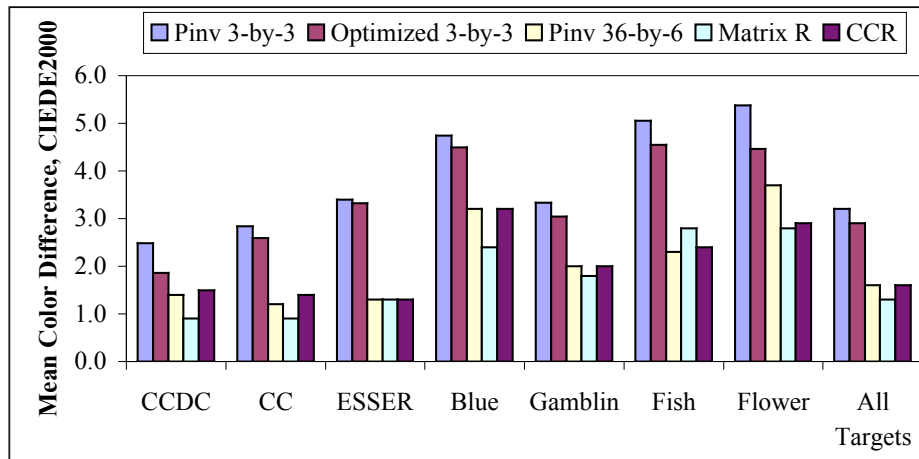


Figure 4 Comparison of mean color difference CIEDE2000 among three spectral imaging methods and two colorimetric imaging methods

For spectral imaging methods, the modified six-channel camera signals were used to estimate spectral reflectance. The spectral % RMS errors are plotted in Figure 5. It was very surprising that the CCR method are achieved the best spectral accuracy for all the targets. CCR method constructs the relationship between spectral reflectances and the extended 21-channels including 6-chanel camera signals and 15 cross product terms. Though the initial information available to CCR and pseudoinverse methods is identical,

those two methods perform differently on spectral reconstruction. Figure 6 plots average spectral difference and one minus correlation coefficient for the calibration target using those two methods, respectively. The pseudoinverse method shows poor correlation between measured and predicted spectral reflectance at short wavelengths. High correlation for CCR method explains why spectral RMS error of CCR method is smaller than that of pseudoinverse method. Although CCR method achieves the best spectral match, it gives no better colorimetric accuracy than the pseudoinverse method.

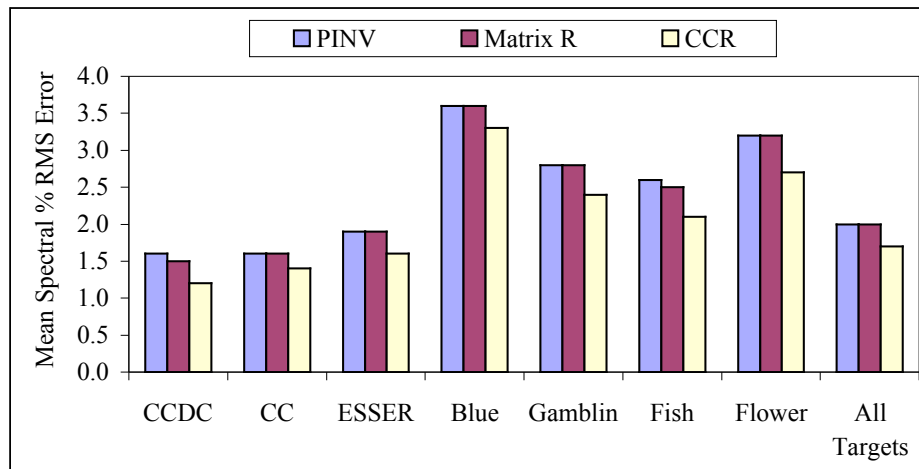


Figure 5 Comparison of mean color difference among the three spectral imaging methods

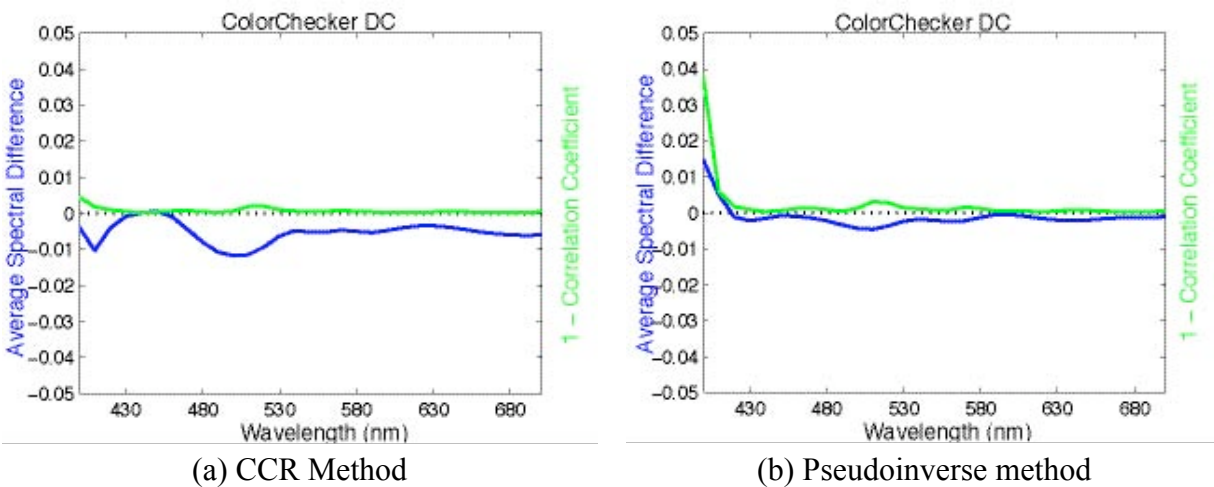


Figure 6 Average spectral difference (blue) and one minus correlation coefficient (green) for GretagMacbeth ColorChecker DC

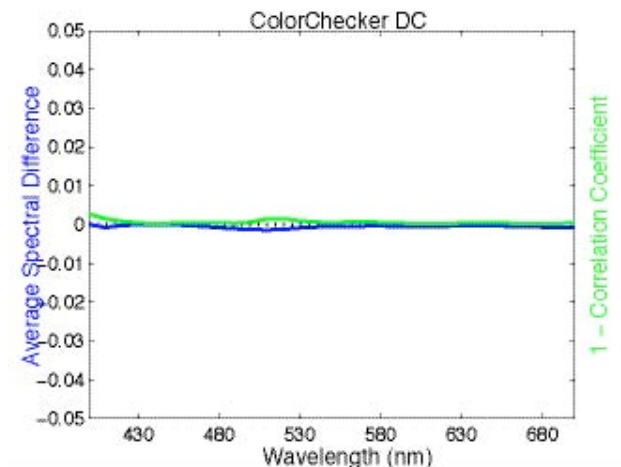


Figure 7 Average spectral difference (blue) and one minus correlation coefficient (green) for GretagMacbeth ColorChecker DC using the pseudoinverse method with extended 21 channels

One might speculate that the result of the pseudoinverse method could be improved if it also incorporates the same 15 cross product terms as in the case for the CCR method. This has been verified by comparing the simulation result in Figure 7 to those in Figure 6. It is obvious that by incorporating the cross product terms, the spectral accuracy of the pseudoinverse method has been significantly improved.

Because the Matrix R method shares the same metameric black as the pseudoinverse method, the spectral RMS error should be similar for these two methods. It also implies that the spectral accuracy of the matrix R method could exceed that of the CCR method if cross product terms are added in the simulation. From Figure 5, it can be seen that spectral RMS error of matrix R method is smaller than that of pseudoinverse method for the CCDC and Fish. Further study should be conducted to understand this result.

## V. Conclusions

The imaging acquisition system – a modified Sinarback 54H coupled with two absorption filters, is by far the most practical spectral system that can achieve spectral color reproduction. It is so simple and easy to incorporate a commercial digital camera with two absorption filters into the current imaging workflow for museums, archives and libraries.

The Matrix R and pseudoinverse methods have a comparable spectral accuracy. When only the six-channel signals are used, the spectral accuracies of those two methods are inferior to that of the CCR method, which uses the extended variable sets to include the 15 cross product terms. However, their accuracies could be improved to even exceed that of the CCR method if they also use the same cross product terms. Among all three methods, the Matrix R method achieved the best colorimetric accuracy for a certain combination of illuminant and observer. The mean color difference for GretagMacbeth ColorChecker DC and ColorChecker was about  $0.9 \Delta E_{00}$ ,  $1.3 \Delta E_{00}$  for ESSER T221, and  $2.8 \Delta E_{00}$  for the two small oil paintings.

The Matrix R method can reach the same spectral accuracy as the pseudoinverse method, and the spectral accuracy of both methods could be improved if they also use the same cross product terms. Furthermore, the Matrix R can achieve the best colorimetric accuracy for a certain combination of illuminant and observer. Thus, the Matrix R is a very promising method for achieving artwork images with sufficient spectral and colorimetric accuracy.

## VI. Reference

1. R. S. Berns, The science of digitizing paintings for color-accurate image archives: a review, *Journal of Imaging Science and Technology*, 4, p305-325 (2001).
2. J. B. Cohen and W. E. Kappauf, Metameric color stimuli, fundamental metamers, and Wyszecki's metamerics blacks, *Am. J. Psychol.* 95, p537-564 (1982).
3. H. S. Fairman, Metameric correction using parametric decomposition, *Color Research and Application*, 12, p261-265, 1997.
4. J. Liang, D. Saunders, J. Cupitt, and M. Benchouika, A new multi-spectral imaging system for examining paintings, *Proc. of the Second European Conference on Color in Graphics, CGIV'2004, Imaging and Vision, Society of Imaging Science and Technology, Springfield, VA, p229-234, 2004.*
5. Alejandro Ribés Cortés, Multispectral analysis and spectral reflectance reconstruction of art paintings, Ph. D. thesis, Dec. 2003, Paris, France.
6. M. Mohammadi, M. Nezamabadi, R. S. Berns, and L. A. Taplin, Spectral imaging target development based on hierarchical cluster analysis, *Proc. Twelfth Color Imaging Conference, Society of Imaging Science and Technology, Springfield, VA, 2004.*
7. F. H. Imai, R. S. Berns, and D. Tzeng, A comparative analysis of spectral reflectance estimation in various spaces using a trichromatic camera system, *Journal of Imaging Science and Technology*, 44, p280-287, 2000.
8. F. H. Imai, Digital camera filter design for colorimetric and spectral accuracy, *Proc. Of the Third International Conference on Multispectral Color Science, University of Joensuu, Finland, pp. 13-16, 2001.*

## Appendix I – Nature of Spectral Reflectance

Spectral reflectance is a physical characteristic of an object surface, while color is nothing but a psychophysical perception that depends on many factors such as the illumination, the observer and surround conditions. Besides, color can be easily deduced from spectral reflectance. So it is more useful to know spectral reflectance of a surface than to know its color. Furthermore it implies that spectral color reproduction, which depicts each scene pixel spectrally, is more powerful than traditional colorimetric reproduction, which represents each pixel colorimetrically.

First, spectral reflectance databases used in the analysis are introduced. Then discrete Fourier transforms are performed on these databases to prove that they are band limited because of the smoothness of spectral reflectance curves.<sup>[1,2]</sup> After that, principal component analysis is used to analyze the databases, and it is found that six eigenvectors can explain almost all the variance. Finally, these databases are plotted on chromaticity diagram to visually study the similarity and dissimilarity between these data sets.

### 1. Spectral Reflectance Databases

There are six targets in the analysis, listed in Table A-1. The spectral reflectance factors of these targets were measured using Macbeth SpectroEye spectrophotometer with 45/0 geometry. The wavelength range was from 380 nm to 730 nm at 10 nm increments.

Table A-1 Lists of the names, abbreviations and number of patches for six targets

No.	Name	Abbreviation	Number of Patches
1	GretagMacbeth ColorChecker DC	CCDC	240
2	GretagMacbeth ColorChecker	CC	24
3	ESSER TE221 scanner target	ESSER	264
4	A custom target of Gamblin conservation colors	Gamblin	60
5	An acrylic-medium blue target	Blue	56
6	Two small oil paintings	Fish & Flower	22

## 2. Fourier Analysis

Generally speaking, spectral reflectance curves are fairly smooth, so they are band limited, which can be proved by performing a Fourier analysis over spectral reflectance databases. For each spectral reflectance factor, its power spectrum can be calculated using Eq. (A-1):

$$\mathbf{S} = [\text{fft}(\mathbf{R}_\lambda, 128)] \times [\text{fft}(\mathbf{R}_\lambda, 128)]^* / 128 \quad (\text{A-1})$$

where  $\mathbf{S}$  is the power spectrum for spectra reflectance factor,  $\mathbf{R}_\lambda$ , symbol  $*$  represents the complex conjugate,  $\text{fft}$  is the abbreviation of fast Fourier transform and  $\text{fft}(R_\lambda, 128)$  means that  $R_\lambda$  is first padded with trailing zeros to length of 128 and then used in a discrete fast Fourier transform.

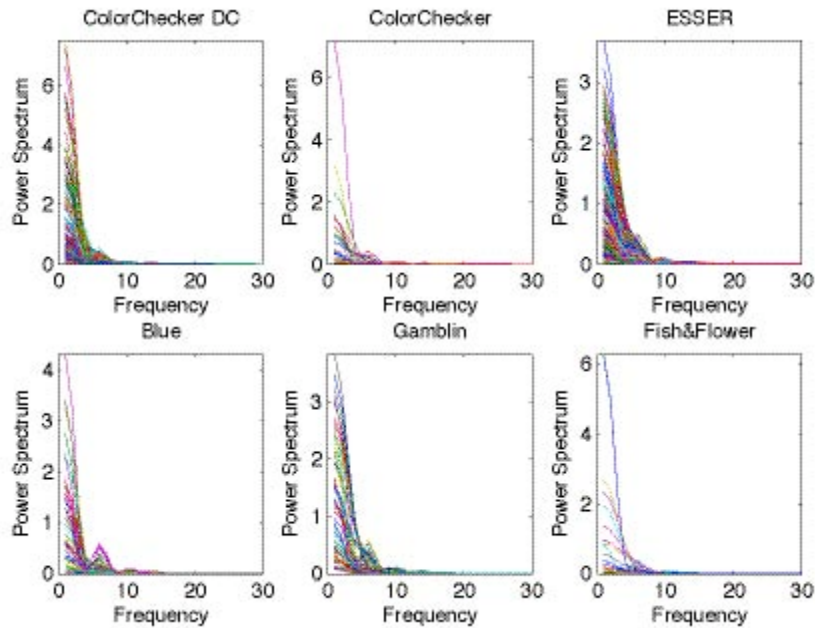


Figure A-1 Power spectra of spectral reflectance factors for six targets

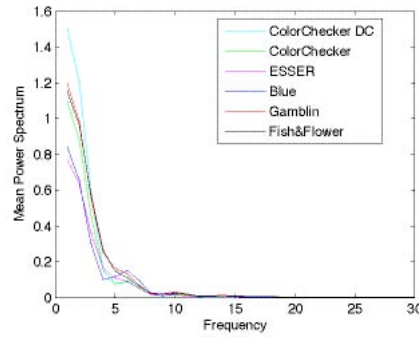


Figure A-2 Mean power spectra for six databases

Figure A-1 shows the power spectra for all the targets. These power spectra are averaged to obtain mean power spectra for each target, shown in Figure A-2. The threshold frequency is defined as the frequency when the value of mean power spectra is smaller than 0.005. There will be nearly no presence of frequency components above the threshold frequency. Table A-2 lists the threshold frequencies for these six targets. It can be easily concluded that these targets are certainly band limited. The smoothness of spectral reflectance curves determines that they are band limited.

Table A-2 Results of Fourier Transform

Data Set	CCDC	CC	ESSER	Gamblin	Blue	Fish & Flower
Threshold Frequency	18	15	12	16	15	18

### 3. Principal Component Analysis (PCA)

Principal component analysis, abbreviated as PCA, is a well-known statistical tool that transforms a number of correlated variables to a small number of uncorrelated variables called principal components. The PCA is used to statistically analyze these databases, and the first six eigenvectors for each database are plotted in Figure A-3.

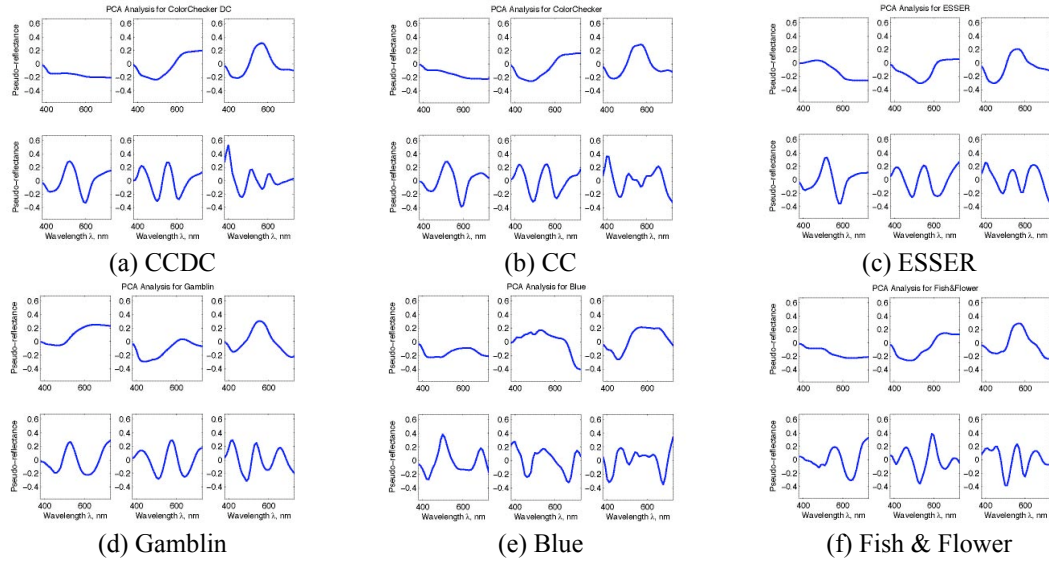


Figure A-3 The first six eigenvectors for each database

From Figure A-3, it can be seen that a certain similarity exists among the eigenvectors of these databases, and that the eigenvectors of blue target are obviously a little different from those of other targets. In spectral imaging, one or two databases are treated as calibration target to build a camera model, while other databases, called independent targets, are transformed to spectral reflectance space according to the model. It is assumed that the model built over calibration target works well for independent targets. The similarity of the first six eigenvectors among these databases satisfies the validity of the assumption. On the other hand, due to the discrepancy of eigenvectors of blue target, it is reasonable to derive that blue target might not be predicted well when the other database is used to generate the model.

Table A-3 lists the % cumulative variance for each database when the number of eigenvectors varies from one to ten. Table A-4 summarizes the number of eigenvectors needed to account for 99% (in zero decimal) or 100.0% (in one decimal) of the total variance. The first six eigenvectors of each database can explain almost 100% (in zero decimal) of the total variance of the database. Thus, the n-dimension spectral reflectance space can be transformed to the 6-dimension eigenvector space with almost 100% accuracy where n accounts wavelength. It also implies that six-channel camera signals are good enough to reconstruct each scene pixel spectrally.

Table A-3 % Cumulative variance for each database

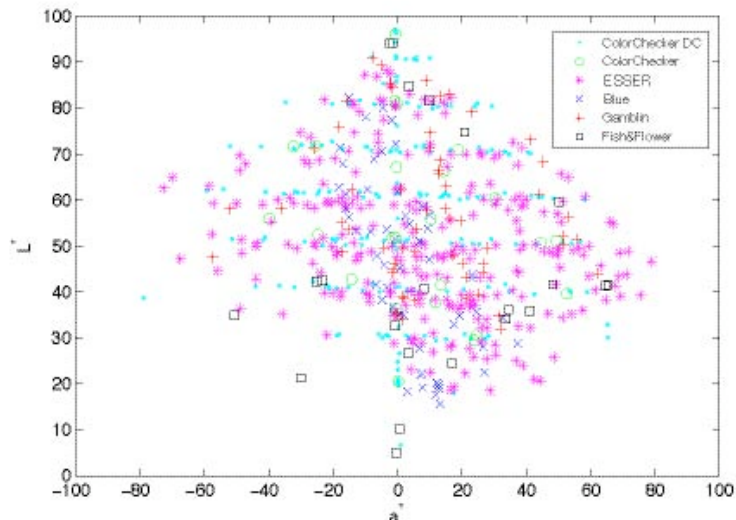
No.	CCDC	CC	ESSER	Gamblin	Blue	Fish & Flower
1	79.6	68.0	70.7	66.8	78.0	72.5
2	95.4	90.9	87.6	87.2	94.4	91.9
3	98.8	98.5	97.3	96.5	98.4	98.1
4	99.5	99.4	98.6	97.9	99.4	99.3
5	99.7	99.7	99.2	99.0	99.7	99.7
6	99.8	99.8	99.5	99.6	99.9	99.8
7	99.9	99.9	99.7	99.7	99.9	99.9
8	99.9	100.0	99.8	99.9	100.0	100.0
9	100.0	100.0	99.9	99.9	100.0	100.0
10	100.0	100.0	99.9	100.0	100.0	100.0

Table A-4 Results of PCA

Database	99% (zero decimal)	100% (in one decimal)
CCDC	3	9
CC	4	8
ESSER	4	11
GAMBLIN	5	10
BLUE	4	8
Fish & Flower	4	8

#### 4. Colorimetric Analysis

The CIELAB values are calculated for the entire database, and plotted in Figure A-4. It can be concluded that ESSER and CCDC occupy a very large volume of CIELAB space, and that blue target locates in such a range that  $a^*$  is between -20 and 20, and  $b^*$  is between -60 and 0. Therefore, both EESER and CCDC database can be the best candidates for calibration targets.



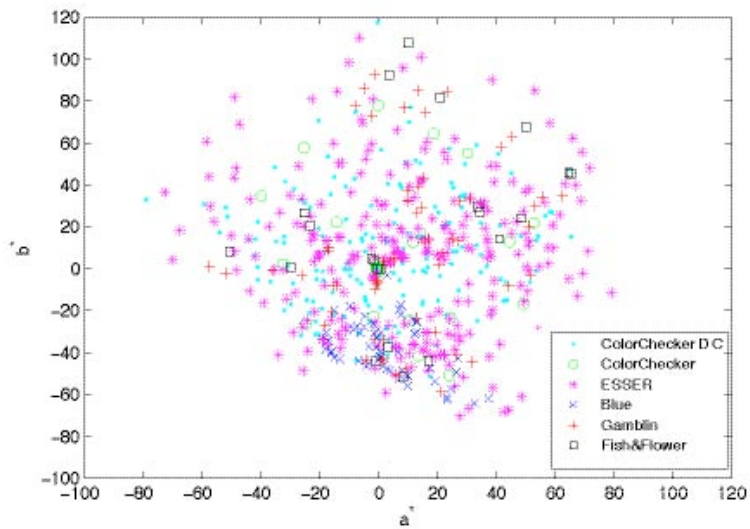


Figure A-4 CIELAB values of all the databases

## 5. Reference

1. W. S. Stiles and G. W. Wyszecki, Counting metameric object colors, J. of Opt. Soc. of American, Vol. 52 (3), p313-328, March (1962).
2. W. S. Stiles, G. W. Wyszecki and N. Ohta, Counting metameric object-color stimuli using frequency-limited spectral reflectance functions, J. of Opt. Soc. of American, Vol. 67 (6), p779-784, June (1977).

## **Appendix II – Canonical Correlation Analysis**

Canonical Correlation Analysis, abbreviated as CCA, seeks to identify and quantify associations between two sets of variables. It maximizes the correlation between linear combinations of variables in one set and linear combinations of variables in other set. First, determine the pair of linear combinations having the largest correlation. After that, determine the next pair having the largest correlation among all pairs uncorrelated with the previously selected pair, and so on. The pairs of linear combinations are called canonical variables and their correlations are called canonical correlations. The maximization characteristic of the statistic method attempts to transform a high-dimensional relationship between two sets of variables into a few pairs of canonical variables.

Although CCA is mainly used for descriptive purposes, it also has some predicative applications. An example is the inverse problem for remote sensing, where the atmosphere effects can be derived from the observed radiation of the airborne or satellite images. <sup>[1,2]</sup> Another possible application in color science is spectral color reproduction, where spectral reflectance factors can be estimated from multi-channel camera signals.

Take spectral color reproduction as an example; some mathematical aspects of CCA will be briefly illustrated. Canonical correlation regression (CCR), whose purpose is to predict one set of variables based on the other set of variables using canonical correlation between them, will be discussed in section 2. Principal component analysis (PCA) is a more common statistical method, and in section 3, it will be compared with CCA. Finally, some conclusions will be drawn in the last section.

## 1. Mathematics of CCA

Given two sets of variables – camera signals,  $\mathbf{X}^{(1)}$ , and spectral reflectance factors,  $\mathbf{X}^{(2)}$ . Camera signals,  $\mathbf{X}^{(1)}$ , are an  $n \times p$  matrix, where  $n$  is the number of patches and  $p$  is the number of channels. Spectral reflectance factor,  $\mathbf{X}^{(2)}$ , are an  $n \times q$  matrix, where  $q$  is the number of wavelengths.

First, calculate the covariance matrix.

$$Cov(\mathbf{X}^{(1)}) = \Sigma_{11}, Cov(\mathbf{X}^{(2)}) = \Sigma_{22}, Cov(\mathbf{X}^{(1)}, \mathbf{X}^{(2)}) = \Sigma_{12}$$

Then perform PCA on the “two big matrices”. Assuming that  $p \leq q$ , the two big matrices share the same  $p$  largest eigenvalues,  $\rho_1^2 \geq \rho_2^2 \geq \dots \geq \rho_p^2$ . Two sets of eigenvectors combine into two matrices.

**E<sub>mat</sub>**– A  $p \times p$  matrix, calculated from the matrix  $\Sigma_{11}^{-1/2} \Sigma_{12} \Sigma_{22}^{-1} \Sigma_{12}^T \Sigma_{11}^{-1/2}$

**F<sub>mat</sub>**– A  $q \times q$  matrix, calculated from the matrix  $\Sigma_{22}^{-1/2} \Sigma_{12}^T \Sigma_{11}^{-1} \Sigma_{12} \Sigma_{22}^{-1/2}$

After that, two sets of canonical variables can be calculated.

$$\mathbf{U}_{mat} = \mathbf{X}^{(1)} \mathbf{A}_{mat} = \mathbf{X}^{(1)} \Sigma_{11}^{-1/2} \mathbf{E}_{mat} \quad (\text{A-2})$$

$$\mathbf{V}_{mat} = \mathbf{X}^{(2)} \mathbf{B}_{mat} = \mathbf{X}^{(2)} \Sigma_{22}^{-1/2} \mathbf{F}_{mat} \quad (\text{A-3})$$

The canonical variables have the following properties. The first pair of canonical variables has the largest correlation, which is equal to the square root of the first eigenvalues, and so on.

$$corr(\mathbf{U}_k, \mathbf{V}_k) = \rho_k, Var(\mathbf{U}_k) = Var(\mathbf{V}_k) = 1$$

$$corr(\mathbf{U}_k, \mathbf{V}_i) = 0, corr(\mathbf{U}_k, \mathbf{U}_i) = 0, corr(\mathbf{V}_k, \mathbf{V}_i) = 0 \text{ When } k \neq j$$

The purpose of CCA is to maximize the correlations between two sets of canonical variables in order to concentrate a high-dimensional relationship between two sets of variables into a few pairs of canonical variables.

## 2. Mathematics of CCR

In previous section, canonical correlation analysis is introduced as a tool to describe the correlations between two sets of variables. It also can be used for predicative purpose in canonical correlation regression. Given one set of variables,  $\mathbf{X}^{(1)}$ , two weight matrices,  $\mathbf{A}\mathbf{mat}$  and  $\mathbf{B}\mathbf{mat}$ , and canonical correlations between two sets of canonical variables,  $\rho_1 \geq \rho_2 \geq \dots \geq \rho_p$ , the other set of variables,  $\mathbf{X}^{(2)}$ , can be estimated. The weight matrices and canonical correlations are preliminarily calculated using two sets of variables for the calibration target.

First, the other set of canonical variables can be predicated using the following equation.

$$\begin{aligned}\hat{\mathbf{V}}\mathbf{mat} &= \mathbf{U}\mathbf{mat} \times \beta_{CC} = \mathbf{X}^{(1)} \times \mathbf{A}\mathbf{mat} \times \beta_{CC} & (\text{A-4}) \\ \beta_{CC} &= \text{diag}(\rho_1, \rho_2, \dots, \rho_p)\end{aligned}$$

Then, the other set of variables can also be estimated.

$$\hat{\mathbf{X}}^{(2)} = \hat{\mathbf{V}}\mathbf{mat} \times \mathbf{B}\mathbf{mat}^{-1} \quad (\text{A-5})$$

The residuals calculated using only  $r$  ( $r < p$ ) pairs of canonical variables are larger than those calculated from the full model using all  $p$  pairs of canonical variables for the calibration target. However, the model using a limited number pairs of canonical variables should be more stable in predicting future values of the independent targets, because the full model is specifically fitted for the calibration target.

## 3. Comparison between CCA and PCA

Principal component analysis is a more useful and common statistical method than CCA. Two methods will be compared in two ways: explained variability and correlation between variables.

Table A-5 and Table A-6 summarizes the variability explained by the first k-th canonical variables and eigenvectors for camera signals and spectral reflectance factors of the calibration target, respectively. It can be noticed that the first canonical variable explains much lower variability than that explained by the first eigenvector, but after including the second canonical variable, the cumulative variability explained is almost as high as that of eigenvectors. Thus, CCA gives the optimal explanation of variability within the subgroup of variables, similar to PCA.

Table A-5 variability explained by the first k-th eigenvectors and canonical variables for camera signals of GretagMacbeth ColorChecker DC

No.	PCA			CCA		
	Variance	% Variance	% Cumulative Variance	Variance	% Variance	% Cumulative Variance
1	0.08	93.37	93.37	0.01	6.87	6.87
2	0.00	5.43	98.80	0.08	90.82	97.69
3	0.00	0.66	99.46	0.00	1.34	99.03
4	0.00	0.45	99.91	0.00	0.06	99.09
5	0.00	0.05	99.96	0.00	0.03	99.12
6	0.00	0.02	99.98	0.00	0.45	99.56
7	0.00	0.01	99.99	0.00	0.03	99.60
8	0.00	0.00	100.00	0.00	0.01	99.60
9	0.00	0.00	100.00	0.00	0.02	99.62
10	0.00	0.00	100.00	0.00	0.13	99.75

Table A-6 Variability explained by the first k-th eigenvectors and canonical variables for spectral reflectance factors of GretagMacbeth ColorChecker DC

No.	PCA			CCA		
	Variance	% Variance	% Cumulative Variance	Variance	% Variance	% Cumulative Variance
1	2.07	79.58	79.58	0.55	21.01	21.01
2	0.41	15.77	95.35	1.91	73.23	94.24
3	0.09	3.45	98.80	0.11	4.41	98.65
4	0.02	0.66	99.47	0.02	0.71	99.36
5	0.01	0.24	99.71	0.01	0.32	99.68
6	0.00	0.11	99.81	0.00	0.07	99.75
7	0.00	0.08	99.90	0.00	0.06	99.81
8	0.00	0.04	99.94	0.00	0.06	99.86
9	0.00	0.03	99.97	0.00	0.05	99.92
10	0.00	0.01	99.98	0.00	0.01	99.92

The correlations between pairs of principal scores can be calculated, and compared with the canonical correlations, as listed in Table A-7. Notice that some correlations have a negative sign, and the absolute values are really important. The correlations between the first two pairs of principal scores are quite high, but the remaining correlations are very low, and the correlations are not monotonically decreasing. On the other hand, the canonical correlations are monotonically decreasing when the negative sign is negligible, and the canonical correlation of the 10<sup>th</sup> pair of canonical variables is still high.

Table A-7 Comparison of correlations between pairs of principal scores and canonical variables for GretagMacbeth ColorChecker DC

No.	1	2	3	4	5	6	7	8	9	10
PCA	0.99	0.97	-0.15	0.03	-0.51	0.27	0.05	-0.02	-0.02	-0.11
CCA	-1.00	-1.00	1.00	1.00	-0.99	0.99	0.96	0.91	-0.89	0.82

CCA can achieve two goals at the same time. One is that CCA gives the maximum correlations between two sets of variables, and the other is that CCA gives the optimal explanation of variability within the subgroup of variables. CCA is significantly superior to PCA by means of the maximum correlations between two sets of variables. However, PCA can be used to reduce the dimensionality of one set of variables and transform these variables into an orthogonal space.

#### 4. Conclusions

Canonical Correlation Analysis deals with two sets of variables and seeks to identify and quantify associations between them. It is mainly used for descriptive purposes, but sometimes for predicative purposes as well. Canonical correlation regression can be used to estimate one set of variables from the other set of variables when two matrices of weights and canonical correlations are obtained from preliminary analysis of calibration target. Both CCA and PCA can give the optimal explanation of variability within one set of variables using a few canonical variables and principal components. Also, CCA can

give the maximum correlations between two sets of variables. Therefore, CCA can achieve two goals at the same time.

## **5. References**

1. Emmett J. Ientilucci, Predicting atmospheric parameters using canonical correlation analysis, Digital Imaging and Remote Sensing Laboratory, internal report.
2. Hernandez-Baquero, E. D. Characterization of earth's surfaces and atmosphere from multispectral and hyperspectral thermal imagery, Ph. D. Thesis, Rochester Institute of Technology, Center for Imaging Science, June, 2000.

## **Appendix III – Paired Comparison Experiment**

The paired comparison method was implemented in a visual experiment. The objective of the experiment was to evaluate one colorimetric imaging method – 3-by-3 matrix and two spectral imaging methods – pseudoinverse and matrix R methods. Five targets were evaluated: the GretagMacbeth ColorChecker DC, The GretagMacbeth ColorChecker, the ESSER TE221 scanner target, a custom target Gamblin conservation colors and an acrylic-medium blue target with a number of different blue pigments.

### **1. Experimental**

A three-channel digital camera, Sinarback 54 digital camera, was tested. The camera was set up approximately perpendicular to the target. The lighting system included two Broncolor HMI F1200 sources, placed at both sides of the camera along the directions 45° away from the line between camera and target. The ColorChecker DC was used as the calibration target to build three camera models under CIE illuminant D65 and 1931 standard observers. The spectral reflectance factors of CCDC were measured using Macbeth SpectroEye spectrophotometer with 45/0 geometry. The nonlinear optimization was implemented for 3-by-3 matrix and matrix R method to minimize the weighted sum of mean and maximum color difference CIEDE2000 between measured and predicted spectral tristimulus values for the calibration target.

A desktop LCD display – IBM T221 was colorimetrically characterized in the dark using a LMT C1210 illuminance colorimeter. Several additional measurements of display colors were measured with the Photo Research PR704 spectroradiometer to transform the LMT measurements to the PR704 by an optimized matrix. Therefore, the complete display profile was based on absolute colorimetry in units of  $\text{cd/m}^2$  for approximate daylight. The radiance of Halon placed on the back wall of a small light booth was measured using PR704 and treated as the rendering illuminant, which approximates to CIE illuminant D50. The camera models were actually built for CIE illuminant D65, so some errors will be introduced due to the difference between D65 and

the rendering illuminant. But the errors are expected to be negligible. At last, the targets were rendered colorimetrically for the rendering illuminant and the 1931 standard observer. These XYZ images were transformed to display digital counts through the LCD inverse model.

The visual experiment was a paired comparison scaling experiment. All the rendering images were 8-bit Tiff and displayed on the IBM T221 display. There were five different targets and three images were generated for each target. For each target, three comparison pairs can then be performed, and repeat this process three times, resulting in nine comparison pairs in total. Apply the same procedure for all five targets. Therefore, each observer compared 45 pairs. Two rendering images were displayed on the desktop LCD with dark background, and the corresponding original target was placed against a blackboard on the back wall of the light booth. Observers were required to select the image from each comparison pair based on colorimetric match to the original target. The experiment was performed in a dark surround. Ten observers participated.

## 2. Results and Discussions

It was assumed that Thrustone's Law of Comparative Judgment (Case V) is valid; that is to say, the dispersions are equal to all the stimuli. The 95% confidence intervals,  $95\%CI$ , were calculated using the following equations:

$$95\%CI = R \pm 1.96\sigma_{pred} \quad (A-6)$$

$$\sigma_{pred} = 1.76(n + 3.08)^{-0.613} (N - 2.55)^{-0.491} \quad (A-7)$$

where  $R$  is the interval scale value,  $n$  is the number of stimuli and  $N$  is the number of observations. The 95% confidence intervals for each target and all the targets are listed in Table A-8, where all the targets mean the combination of all five targets. The total number of observations for each target and all the targets is 30 (repeat 3 times and 10 observers) and 150 (repeat 3 times, 10 observers and 5 targets), respectively, which explains why 95% confidence interval for all the targets is smaller than that for each target.

Table A-8 Experimental Results of the interval scale values and the 95% confidence intervals for each target and all the targets

Target	CC	CCDC	ESSER	Gamblin	Blue	All the Targets
3-by-3 Matrix	-0.98	-1.22	-0.82	-1.22	-0.93	-0.98
Pseudoinverse	0.26	0.72	0.47	0.53	0.43	0.46
Matrix R	0.72	0.50	0.35	0.70	0.50	0.52
95% CI	0.22	0.22	0.22	0.22	0.22	0.10

Figure A-5 shows the interval scale values with 95% confidence intervals for each target and all the targets. It can be concluded that two spectral imaging methods – pseudoinverse and matrix R methods are significantly better than colorimetric imaging method – 3-by-3 matrix, and that they are not significant different from each other. It is not surprising that spectral imaging is superior to traditional colorimetric imaging, since additional three-channel camera signals are used to define the targets spectrally. More useful information is added into the system, and the performance should be improved according to information theory. Compared with the pseudoinverse method, the matrix R method includes an extra step which transforms camera signals to tristimulus values using GOG model and an optimized  $3 \times 6$  matrix. Based on simulation results, colorimetric accuracy of the matrix R method is better than that of the pseudoinverse method for both CC and CCDC. However, matrix R method was significantly better than the pseudoinverse method for only the CC in this visual experiment. One possible reason is that since there are only 24 patches in the ColorChecker; it was easy for an observer to pick a reproduced image more like the original target. The observers commented that the visual task was the easiest for the CC, and the hardest for the CCDC (240 patches) and the ESSER (283 patches). The possible solution is to perform paired comparison of selected simple patches from all the targets, because it is much easier to compare two simple patches with related original patch than complex targets.

### 3. Conclusions

The results show two spectral imaging methods are significantly better than colorimetric imaging method, and that they are not significantly different from each other. The result is quite reasonable. The additional three channels can facilitate accurate tristimulus

estimation and provide the possibility of spectral color reproduction for each scene pixel. It is very promising that the matrix R method is significantly better than the pseudoinverse method for the ColorChecker. One possible reason why the two spectral imaging methods are not significant different from each other is that the complexity of the targets except for the ColorChecker influences the observers' judgments.

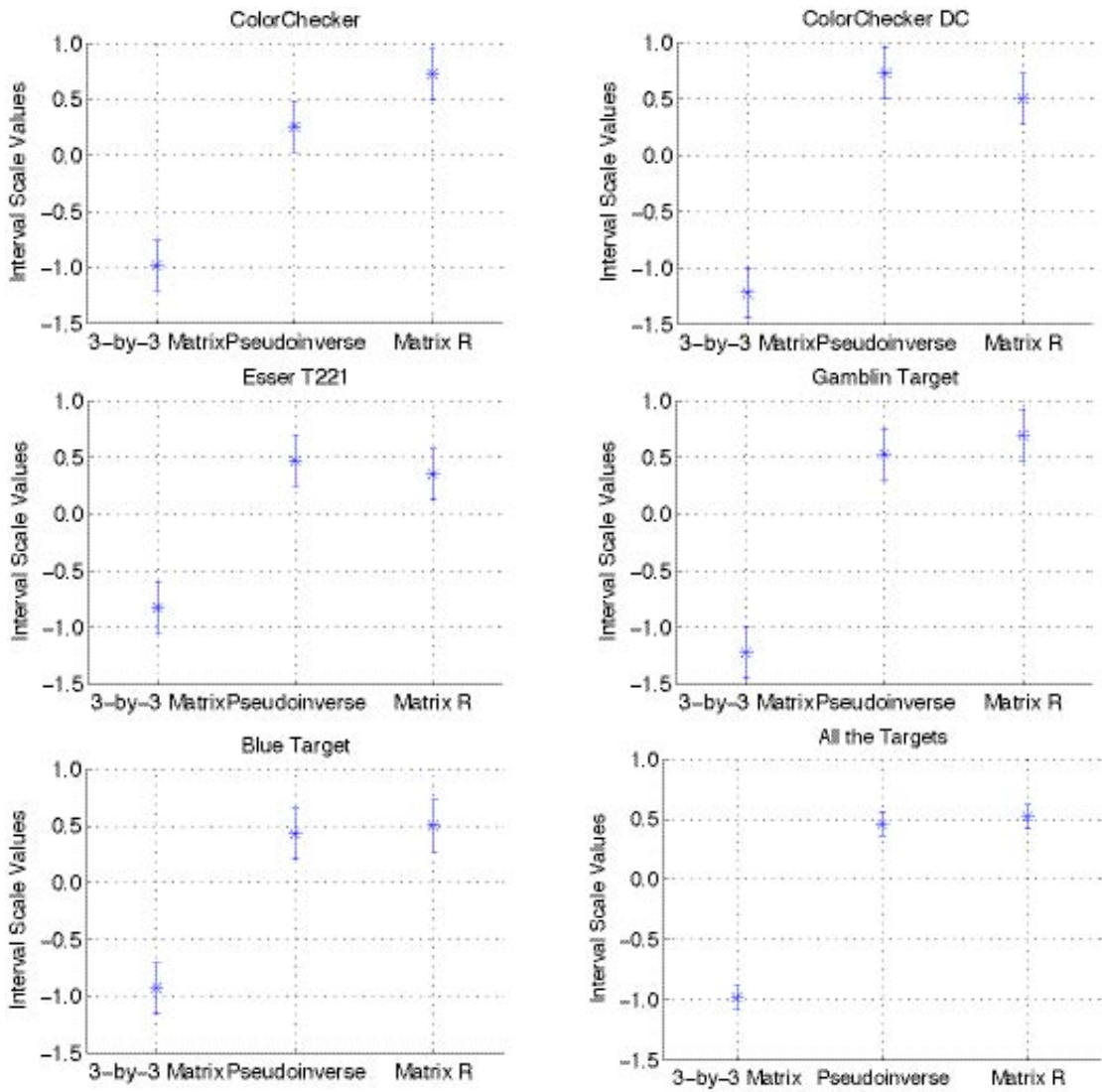


Figure A-5 Results of paired comparison experimental